Identification of High-Speed Moving Loads using Weakened Modal Shape Functions Conceptualised by the Dynamic Influence Line

Afshin Moslehi Tabar[1*], Konstantinos Daniel Tsavdaridis[2*], Miguel Bravo-Haro[2]

[1] Department of Civil Engineering, Tafresh University, 3951879611, Tafresh, Iran

[2] Department of Engineering, School of Science & Engineering, City, University of London, Northampton Square, EC1V 0HB, London, UK

*Corresponding Author (Konstantinos.Tsavdaridis@city.ac.uk)

Abstract

Identification of moving loads is an inverse problem which is important for the lifespan evaluation of bridges. One of the challenging features is to overcome the ill-conditions commonly involved in the inverse problems. In this paper, the ill-conditions are significantly degraded using weakened modal shape functions conceptualised by the dynamic influence line. Employing the main concept of Muller-Breslau's principle, a surrogate beam is developed by eliminating the required reaction. It is replaced by a dynamic load proportional to the modal shape functions of the surrogate beam; not those of the original beam. In this condition, the main source of singularities is eliminated. Consequently, the results obtained by the proposed method provide smooth curves that fit well to the exact solutions without any extra fluctuations which harden the load identification. The results obtained from the case studies show that the loads identified by the proposed method agree well with the exact solutions, although only the first shape function of the surrogate beam was involved.

Keywords: Moving load identification; high speed loads; weakened shape functions; dynamic influence line; DIL

1. Introduction

Monitoring a vehicle load passing a bridge is an important task for the assessment of the bridge health conditions [1]. The load identification gets more importance as the demand to use higher speed vehicles and heavier truck-train loads is growing up. These two features can deteriorate the health conditions of the existing bridges due to the fatigue phenomenon. Traditional methods measure the gross static load of vehicles. In these methods the vehicle is required to pass through a device line with a limited speed. However, for higher speeds, the dynamic effects of the problem rise, and static evaluation methods cannot be reliable.

In recent decades, many researchers have developed methods to identify moving loads based on the inverse problems in the field of structural dynamics, well reviewed by Yu and Chan [2]. The pioneering attempt in this line was carried out by O'Connor and Chan [3], introducing a method for load identification named Interpretive Method I (IMI) by which the vehicle-bridge interaction forces are measured from the bridge total responses. In this method, the bridge is assumed to be a series of lumped masses interconnected by massless elastic beam elements. This method was improved by Chan et al. [4] using Euler-Bernoulli beam model and modal analysis to interpret the dynamic loads. Law et al. [5] developed the Time Domain Method (TDM) using the time-domain analysis. The time-domain analysis method was used to analyse the bridge deck as a simply supported Euler-Bernoulli beam under the vehicle/bridge interaction forces as one-point or two-point loads. Since then, TDM was promoted using the Fourier transformation and the frequency time-domain method (FTDM) was developed [6,7]. In FTDM, the axle load identification is conveniently upgraded using the Fourier transformation of the load response and the method of least squares. Moreover, different promotions have been adopted to better identify the moving loads using different fitting functions and introducing more convenient integration methods [8,9,10].

The inverse solutions mentioned above have an intrinsic weak point. The inversion of the structural matrices suffers from ill-condition problems [11]. Pinkaew [12] utilised an updated static component technique to promote the accuracy of the identified loads. González et al. [13] introduced an algorithm based on first-order Tikhonov regularisation to identify the moving forces. In this direction, research has been performed to mitigate ill-condition problems by using different regularisation methods [14-19]. Li et al. [20] developed a hybrid LSQR algorithm to improve the ill-posedness of the inverse problem solved by the time domain analysis. Chen et al. [21] carried out a comparative study of the criteria for regularisation parameter selection. Some researchers utilised the Singular Value Decomposition (SVD) method [22], however, it commonly requires excessive computation process for regularisation, motivating some researchers to improve the SDV method. Using truncated methods to make SVD less sensitive to noise are efficient

solutions [23,24]. Furthermore, the abilities of the artificial neural network (ANN) in pattern recognition and optimisation have become another reliable tool in the field of load identification [25,26].

According to the state-of-the-art review carried out by Paul and Roy [27] in the field of the bridge weigh-in-motion (B-WIM), the bridge influence line in any form plays a vital role as the main background of bridge health monitoring methodologies. During the initial practice of first-generation B-WIM system, Moses [28] used theoretical static influence line which estimates the gross vehicle weight rather accurately. Past studies have confirmed that the bending moment responses are independent to noises as compared to the acceleration responses [29]. Consequently, many researchers have taken the moment influence line as a base for identification of moving loads. Wang et al. [30] employed influence lines to fit dynamic strain for identification of axle loads. The influence line is also used for damage detection [31,32]. Using the influence line principle, the transverse distribution of the moving load was studied by Yang et al. [33]. Qian et al. [34] reduced the singularity and ill-conditioned matrix by involving the inertial effects in the definition of the dynamic moment. The proposed approach utilising the influence lines of bending moment for the moving load identification showed high effectiveness.

In the aforementioned methods, the main approach is based on the mathematical solutions existing in the field of linear Algebra or numerical computations to mitigate the singularity problems. Whereas this paper aims to overcome the singularity consequences by means of a structural engineering concept, i.e., the influence line (IL). Albeit the IL was originally developed in the field of structural statics assuming the moving load velocity is negligible, the concept was promoted to the dynamics, called the dynamic influence line (DIL), to take the inertia sources and the velocity into consideration [35,36]. In this paper, the DIL method is employed to replace the bridge-vehicle dynamic problem with a surrogate structural system under a dynamic point load. The structural shape functions of the surrogate structure and the assumed dynamic load function are weakened so that the source of singularities is eliminated. Although this process reduces the accuracy of the identified loads to some extent, it is simple and convenient for practical purposes. It is worth mentioning that the proposed method is herein implemented for the load identification, however, it can be utilised in the field of the damage detection in which the response of specific members of a structure should be determined. Furthermore, it should be noted that the present method works based on the external and internal reactions which can be monitored by proper setting of strain gages, using longitudinal gages at the bottom face of the beam for evaluation of the beam moment or using rosette strain gages for identification of the shear.

2. Development of the proposed load identification method

To describe the main concept of the proposed method, a single moving load, P, is considered to pass along a multi-span beam with a constant speed v, as shown in Fig. 1. This case is indeed simulating a multi-span bridge super-structure subjected to a moving load in a simple way. The beam deformation and the distance of the load P at any given time are denoted by $y(x,t)$ and $\xi(t)$, respectively.
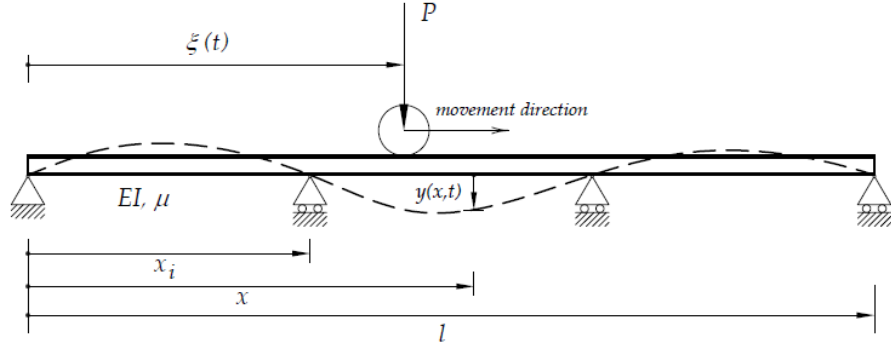
Fig. 1. Specification of a multi-span beam under a moving load

By using modal decomposition method, the deformation of the beam shown in Fig. 1 is evaluated as follows:

$$y(x,t) = \sum_{i=1}^{\infty} \phi_i(x)\, \eta_i(t) \tag{1}$$

where ϕ_i is the modal shape functions of the beam, and η_i is the corresponding modal generalized coordinate.

Given y(x,t), the internal moment and shear actions can be obtained as follows:

$$M(x,t) = EI \sum_{i=1}^{\infty} \frac{d^2}{dx^2} \phi_i(x)\, \eta_i(t) \tag{2}$$

$$V(x,t) = EI \sum_{i=1}^{\infty} \frac{d^3}{dx^3} \phi_i(x)\, \eta_i(t) \tag{3}$$

As an alternative method to determine the variation of an arbitrary external or internal reaction (like the reaction of the j-th support) during the time of passing, the superposition principle is employed, as shown

4

in Fig. 2. Indeed, the original structure shown in Fig. 1 is decomposed into a surrogate structure under two different loading conditions, as shown in Fig. 2. According to the superposition principle, the composition of the structures shown in Figs. 2(a) and 2(b) is equivalent to the original structure providing that the reaction of the j-th support (shown in Fig. 2b) neutralises the deformation at the j-th support position of Fig. 2(a) induced by the load P moving along the beam.
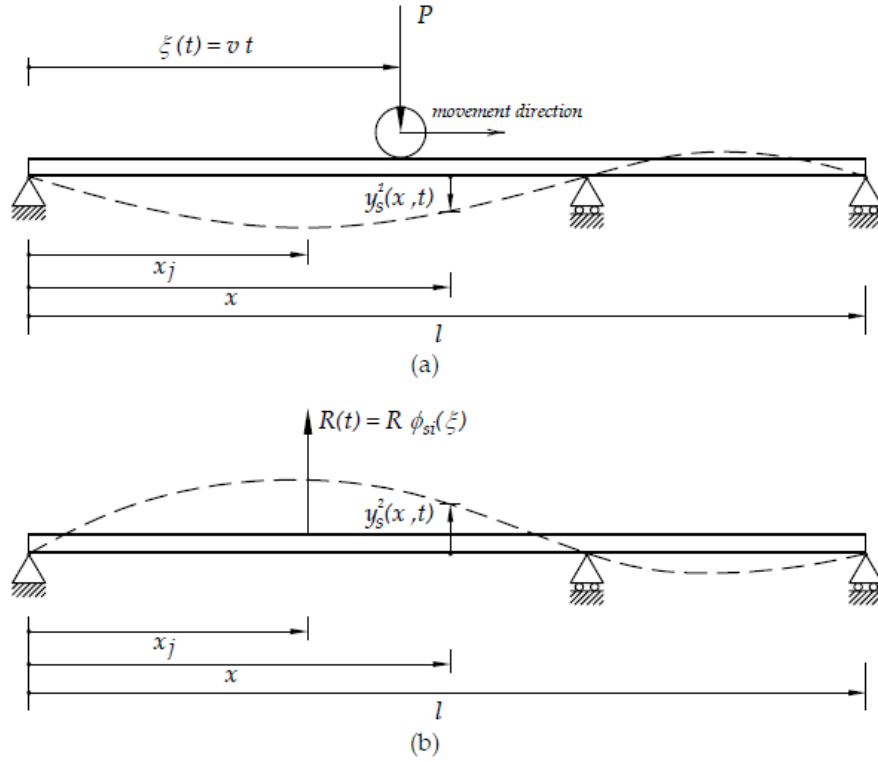
Fig. 2. Surrogate beam induced by eliminating a reaction

With the elimination of a reaction, a surrogate structure is developed so that the order of its modal shape functions, ϕ_{si}, is weakened as compared to that of the original structure, i.e., ϕ_i.

In this condition, the deformation of the surrogate beam shown in Fig. 2(a) is evaluated as follows:

$$y_s^{(1)}(x,t) = \sum_{i=1}^{\infty} \phi_{si}(x)\, \eta_{si}^{(1)}(t) \tag{4}$$

5

where $\eta_{si}^{(1)}$ is the modal generalised coordinate of the surrogate beam shown in Fig. 2. Since the force acting on the beam is a moving concentrated load located at $\xi(t)$, it can be defined as below:

$$q_s^{(1)}(x, t) = P\, \delta(x - \xi) \tag{5}$$

in which δ is the delta-Dirac function. The generalised force corresponding to the i-th mode can be determined as:

$$Q_{si}^{(1)}(t) = P \int_0^l \phi_{si}(x)\, \delta(x - \xi)dx = P\, \phi_{si}(\xi) \tag{6}$$

By using the Duhamel's integral, the generalised coordinate for the i-th mode is obtained as:

$$\eta_{si}^{(1)}(t) = \frac{P}{\omega_{si}} \int_0^t Q_{si}^{(1)}(\tau)\, \sin \omega_{si}(t - \tau)\, d\tau \tag{7}$$

in which ω_{si} is the natural frequencies of the surrogate beam.

Now, it is assumed that the surrogate beam is subjected to the load $R(t) = R\, \phi_{si}(\xi)$ at the j-th support as shown in Fig. 2(b). Accordingly, the deformation of the surrogate beam is derived as follows:

$$y_s^{(2)}(x, t) = \sum_{i=1}^{\infty} \phi_{si}(x)\, \eta_{si}^{(2)}(t) \tag{8}$$

in which $\eta_{si}^{(2)}$ is the modal generalised coordinate of the surrogate beam shown in Fig. 2(b). Since the force acting on the beam is a concentrated load located at x_j, it can be defined as below:

$$q_s^{(2)}(x, t) = R\, \phi_{si}(\xi)\, \delta(x - x_j) \tag{9}$$

The generalised force corresponding to the i-th mode can be determined as:

6

$$Q_{si}^{(2)}(t) = R \int_0^l \phi_{si}(x)\, \phi_{si}(\xi)\, \delta(x - x_i)\, dx = \beta_{si} Q_{si}^{(1)}(t)$$

(10)

in which

$$\beta_{si} = \left(\frac{R}{P}\right) \phi_{si}(x_i)$$

(11)

Then, the modal generalised coordinate of the surrogate beam shown in Fig. 2(b) is derived as:

$$\eta_{si}^{(2)}(t) = \frac{\beta_{si} P}{\omega_{si}} \int_0^t Q_{si}^{(1)}(\tau)\, \sin \omega_{si}(t - \tau)\, d\tau$$

(12)

Now, comparing Eq. (12) to Eq. (7), the following relationship is developed between $\eta_{si}^{(1)}$ and $\eta_{si}^{(2)}$:

$$\eta_{si}^{(2)}(t) = \beta_{si}\, \eta_{si}^{(1)}(t)$$

(13)

This proves that the generalised coordinate of the surrogate beams shown in Figs. 2(a) and 2(b) are proportional to each other only if the concentrated load $R(t)$, imposed in Fig. 2(a), is proportional to the modal shape functions of surrogate beam. In other words, choosing $R(t) = R\, \phi_{si}(\xi)$ is true. Furthermore, the same method can be implemented for the moment reactions, except that the surrogate beam is obtained by eliminating the required internal moment. As an example, the surrogate beam needed to evaluate the DIL of the internal midspan moment is shown in Fig. 3.
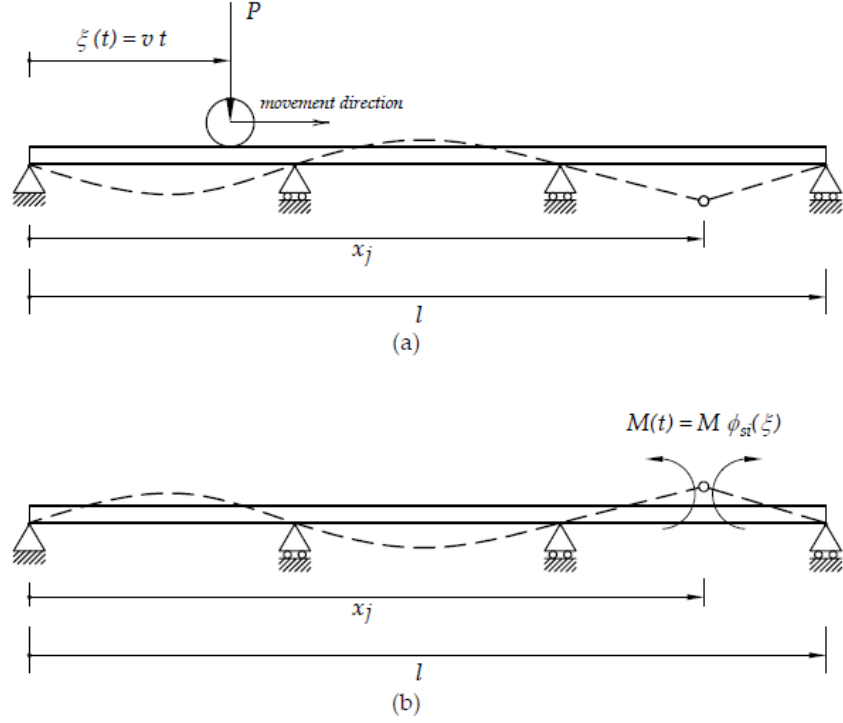
Fig. 3. Surrogate beam for internal moment influence line

In this case, the slopes induced in the surrogate beams shown in Figs. 3(a) and 3(b) should neutralise each other. Accordingly, the slopes are needed to find as follows:

$$\frac{dy_s^{(1)}}{dx}(x,t) = \sum_{i=1}^{\infty} \frac{d\phi_{si}}{dx}(x)\, \eta_{si}^{(1)}(t) \tag{14}$$

$$\frac{dy_s^{(2)}}{dx}(x,t) = \sum_{i=1}^{\infty} \frac{d\phi_{si}}{dx}(x)\, \eta_{si}^{(2)}(t) \tag{15}$$

In addition, the generalised force corresponding to the *i*-th mode of the beam shown in Fig. 3(b) is determined as:

$$Q_{si}^{(2)}(t) = M \int_0^l \frac{d\phi_{si}}{dx}(x)\frac{d\phi_{si}}{dx}(\xi)\, \delta(x - x_i)\, dx$$

$$= M\, \frac{d\phi_{si}}{dx}(x_i)\, \frac{d\phi_{si}}{dx}(\xi) \tag{16}$$

8

Finally, Eqs. (12) and (13) imply that any reaction of the original beam during the time, or the influence line in other words, is equivalent to the variation of the corresponding deformation of the beam while subjected to the force $R(t) = R\ \phi_{si}(\xi)$ which is proportional to the surrogate beam deformation. This finding agrees with the main concept of the Muller-Breslau's principle.

The merit of this finding in the field of the moving load identification is that the singularity sources, existing near the location of the required reaction, are eliminated by using a weakened form of the modal shapes of the surrogate beam. Furthermore, the modal shape functions used in the present method belong to the surrogate structure which are of lower order, making the computations much simpler and faster.

It should be noted that the proposed method is based on the Euler beam theory. However, the general finding of the theory may be adopted to more complicated beam theories in which the shear deformation or any sources of inhomogeneity, porosity, composite action, nonlinearity and cracks are involved [37-42]. For this purpose, the key task is to find modal shape functions of the surrogate beam in presence of the desired effects. This can be performed either by beam theories or other methods such as FEM.

3. Validation of the proposed method

The validity of the proposed method is examined by means of examples described in this section. In the first two parts, the accuracy of the method in the structural analysis is evaluated for a single load (a simpler problem), moving on both statically determinate and indeterminate structures. Indeed, the application of the theory is generally the same for both cases, except that in the statically determinate structures, the surrogate structure consists of some unstable members with only one mode of vibration. This makes the analysis of the statically determinate structures much easier. Since many of bridges are statically determinate the proposed method may be applied conveniently. Moreover, the feasibility of the proposed method is verified by comparing its results with a test data obtained by Yang et al. [24] in Example 4.

3.1. Statically determinate structures

3.1.1. Example 1

A simply supported 20 m long beam is considered as shown in Fig. 4. A concentrated load P passes along the beam with constant speed of 40 m/s (144 km/h). The variation of the reaction of the support B and the mid-span moment is evaluated.

P	E (GPa)	I (m⁴)	μ (kg/m)	l (m)
	200	9.21x10⁻³	400	20.0
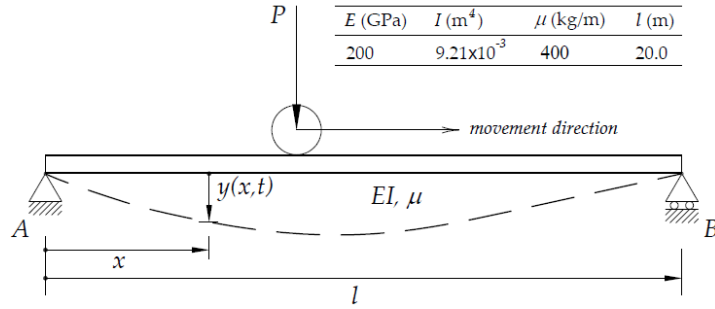
Fig. 4. Specification of simply supported beam

For determining the reaction at the support B and the moment at the mid-span using the proposed method, the exact sinusoidal modes of vibration of a simple span beam in the form of $\sin\frac{n\pi x}{l}$ are converted to the linear ones as shown in Figs. 5(a) and 5(b) for the support B reaction and the mid-span moment, respectively. Accordingly, not only the exact shape functions are weakened to linear ones, but the infinite number of the modes are reduced to only one mode in this beam as a statically determinate structure.

(a)

(b)
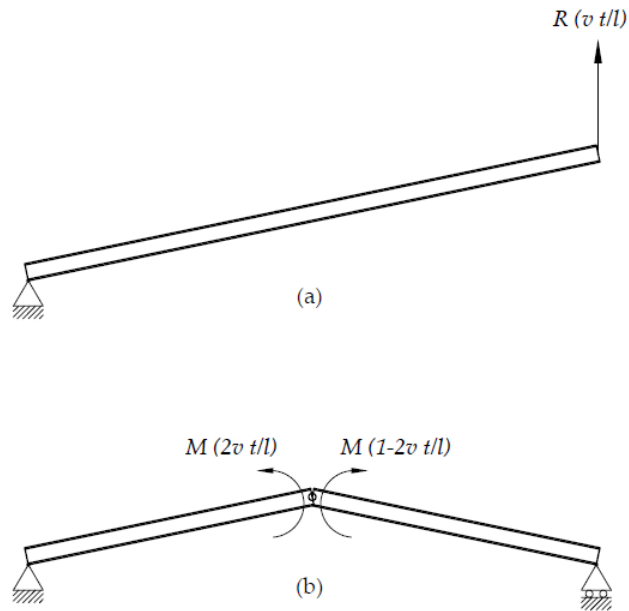
Fig. 5. Surrogate beams for determination of: (a) the support B reaction; (b) the mid-span moment

The goal is to investigate the accuracy and the efficiency of the proposed method as compared with the exact nonlinear solution and the modal decomposition method. For the exact solution, the capability of SAP2000 [43] software in the modelling of moving load was used based on the nonlinear time-history analysis. Moreover, the modal decomposition method has a well-known solution coming from the field of

10

structural dynamics [44] in which the deflection of a simple supported beam under a moving load is obtained as below [44]:

$$y(x,t) = \frac{2Pl^3}{EI\pi^4} \sum_{i=1}^{\infty} \frac{1}{n^4} \frac{1}{1-(\omega_0/\omega_i)^2} \sin\frac{n\pi x}{l} \left(\sin\omega_0 t - \frac{\omega_0}{\omega_i} \sin\omega_i t \right) \tag{17}$$

Consequently, the reaction of support B and the mid-span moment of the beam can be derived as follows:

$$R_b(l,t) = \frac{2P}{\pi} \sum_{i=1}^{\infty} \frac{(-1)^i}{i} \frac{1}{1-(\omega_0/\omega_i)^2} \left(\sin\omega_0 t - \frac{\omega_0}{\omega_i} \sin\omega_i t \right) \tag{18}$$

$$M(x,t) = -\frac{2Pl}{\pi^2} \sum_{i=1,3,5,\dots}^{\infty} \frac{(-1)^i}{i^2} \frac{1}{1-(\omega_0/\omega_i)^2} \left(\sin\omega_0 t - \frac{\omega_0}{\omega_i} \sin\omega_i t \right) \tag{19}$$

To assess the efficiency of the method in comparison to the modal decomposition method, the reaction and the mid-span moment, introduced by Eqs. (18) and (19), were evaluated with different number of modes (1,5,10,15,20,50,100). The reaction of support B is normalised by the load P as shown in Fig. 6. As observed, the method could trace the exact nonlinear solution with an acceptable smooth curve without fluctuation. On the other hand, in the classic modal decomposition, a lot of modes should be involved to reach an acceptable accuracy.
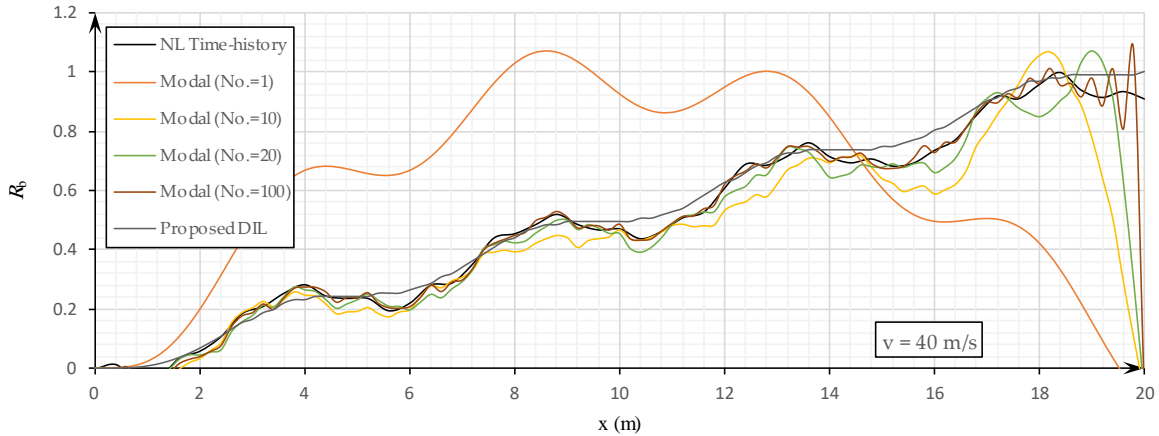
Fig. 6. Variation of the support B reaction during the load passage

To assess the differences in detail, the error of the evaluated reaction in different locations (L/5, 2L/5, L/2, 3L/5 and 4L/5) with respect to the exact nonlinear solution is given in Table 1. The accuracy in the regions

near the end support is lower because of the inertial forces acting at the beginning of vibration and the ending free vibrations. As observed, the present method provides relatively accurate estimations at the middle parts of the beam (2L/5 to 3L/5) when considering only one mode. It is worth noting that in the modal decomposition method more than 20 modes of vibration are required to reach desirable accuracy, taking 0.0025-s CPU time [Intel(R) Core(TM) i7-7600U CPU @ 2.80GHz   2.90 GHz]. The time elapsed for the present DIL is approximately 0.0008 s, i.e., one third of that needed for the modal analysis.

The same investigation was carried out for the mid-span moment. The results are shown in Fig. 7 and Table 2. In Fig. 7, the moments were normalised by the maximum static moment (PL/4). The results prove that the present method has good accuracy despite its simplicity.

Table 1. Error in support B reaction with respect to nonlinear time-history analysis (%)

Method	No. of modes	Measurement location				
		L/5	2L/5	L/2	3L/5	4L/5
Modal	1	135.3	125.7	95.9	55.5	32.9
	10	13.0	13.7	0.9	12.6	20.1
	20	6.7	7.2	3.8	5.2	10.5
	100	2.7	1.2	3.3	2.2	1.0
Present DIL	1	18.6	3.6	4.8	2.7	8.9
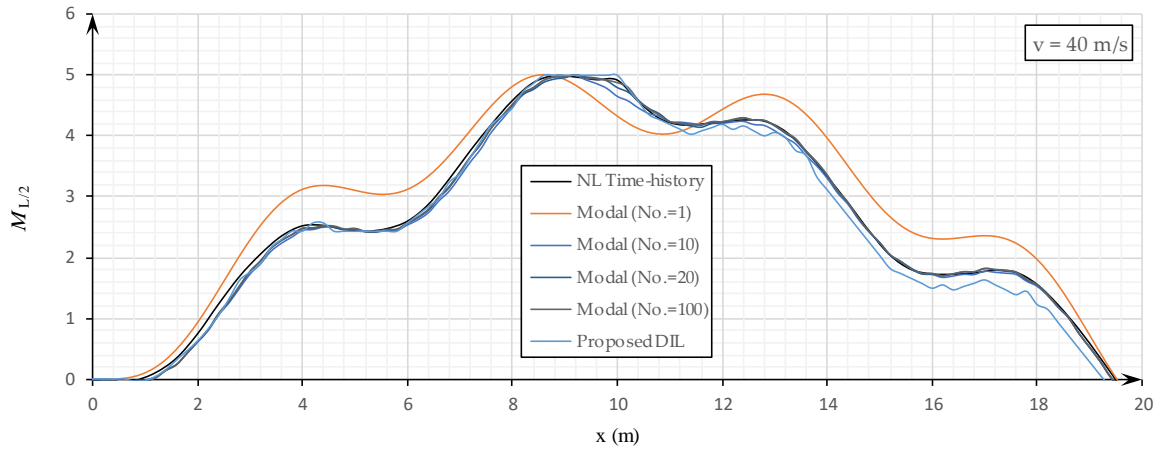
Fig. 7. Variation of the mid-span moment during the load passage

Table 2. Error in mid-span moment with respect to nonlinear time-history analysis (%)

Method	No. of modes	Measurement location				
		L/5	2L/5	L/2	3L/5	4L/5
Modal	1	23.2	4.7	12.3	4.5	33.0
	10	3.1	2.4	5.5	0.6	0.7
	20	2.1	1.9	2.7	0.8	0.3
	100	1.8	1.6	1.1	0.2	0.2
Present DIL	1	3.8	2.8	1.5	1.2	14.1

In addition, the sensitivity and accuracy of the proposed method in terms of various speed of the moving load is studied. Herein the moving load is considered to pass along the simple support beam with speed of 20, 40 and 80 m/s (72, 144 and 288 km/h, respectively). The results for the reaction at the support B and the moment at the mid-span are illustrated in Figs. (8) and (9), respectively. Similarly, the proposed method showed acceptable estimation of the actions. The corresponding curves are smooth without extra fluctuation which eases the load identification process in comparison to the modal decomposition method in which load identification is complicated due to the excessive number of modes required. It should be noted that the first 20 modes of vibration have been involved in the modal decomposition method while only one mode provides adequate accuracy in the present DIL method.

Moreover, in Figs. (8) and (9), the static influence line is also shown. The comparison between similar curves obtained by the proposed method and the static influence line reveals how the inertia sources, i.e., moving load velocity and mass, affect the structural responses. This difference is much more noticeable for the loads with higher speeds.
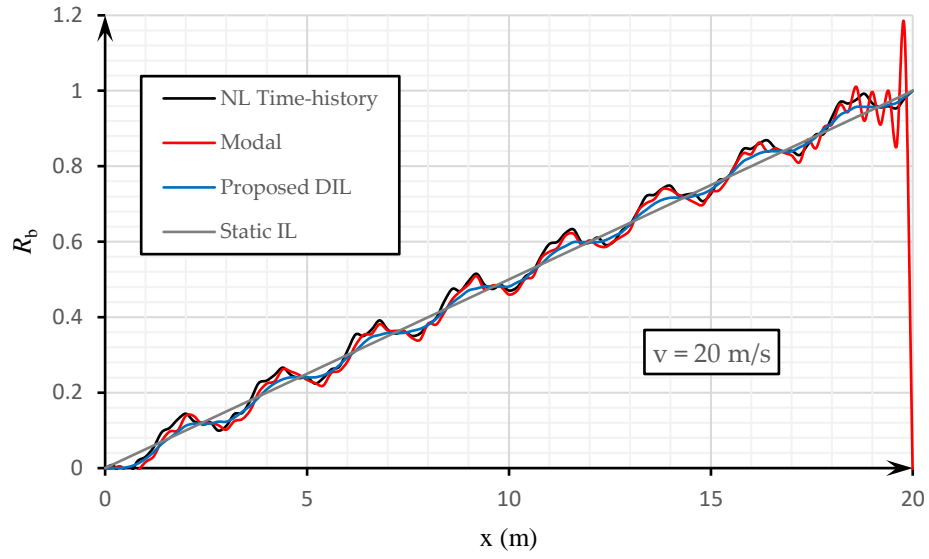
(a)
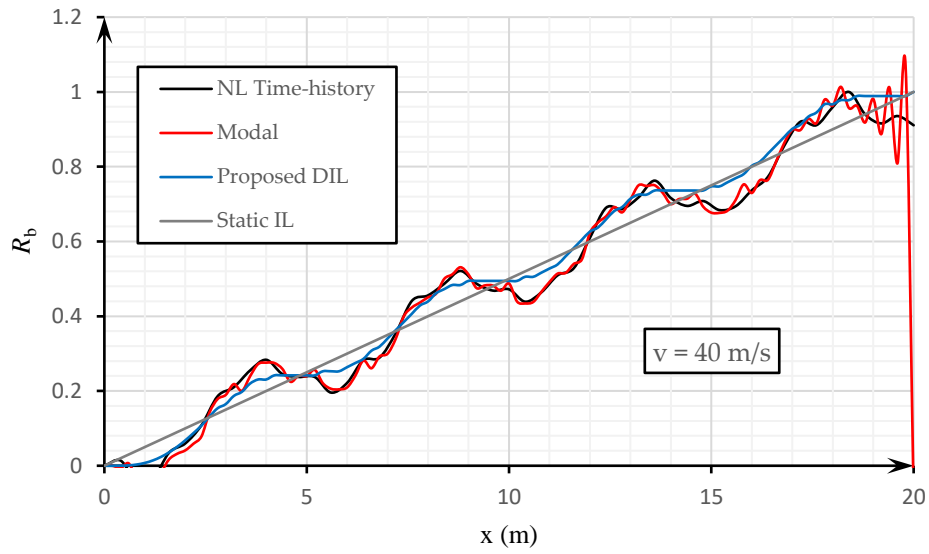
(b)
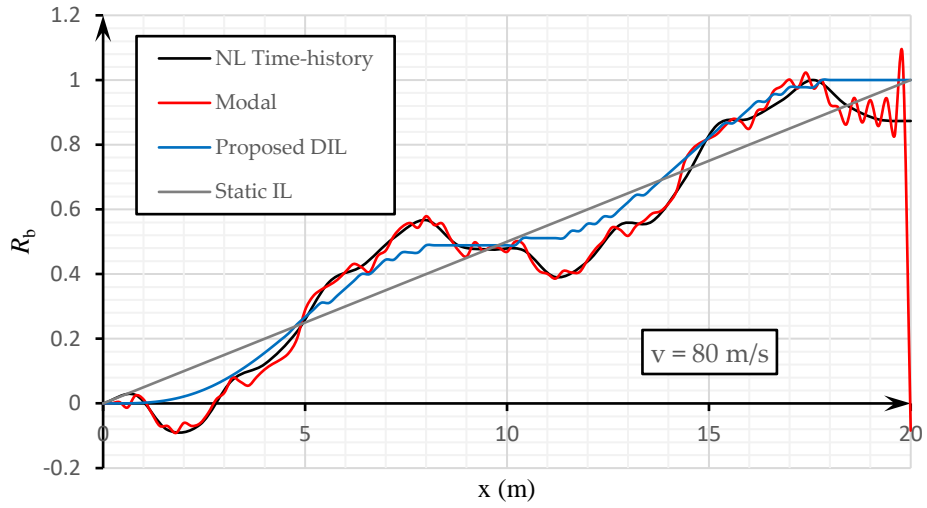
(c)

Fig. 8. Variation of the support B reaction during the load passage with the speed of: (a) 20 m/s; (b) 40m/s; (c) 80 m/s
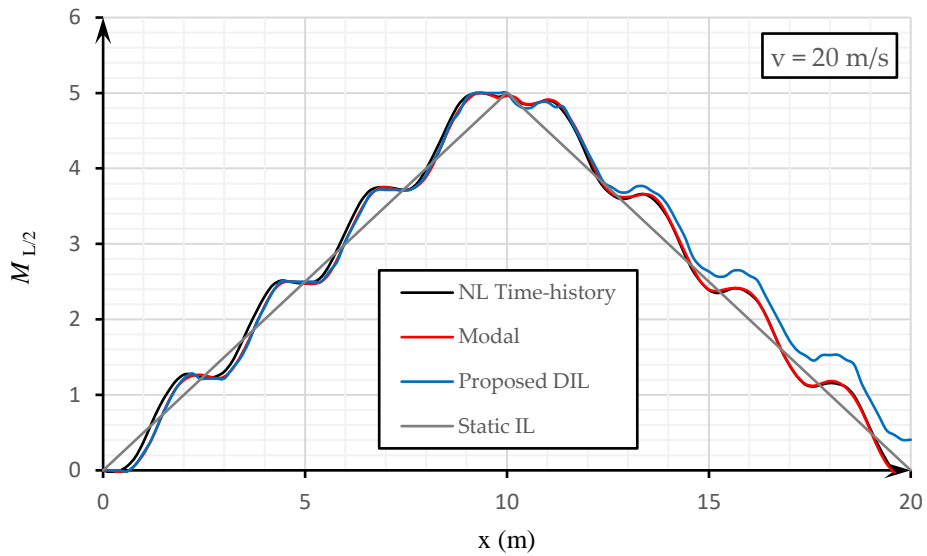
(a)
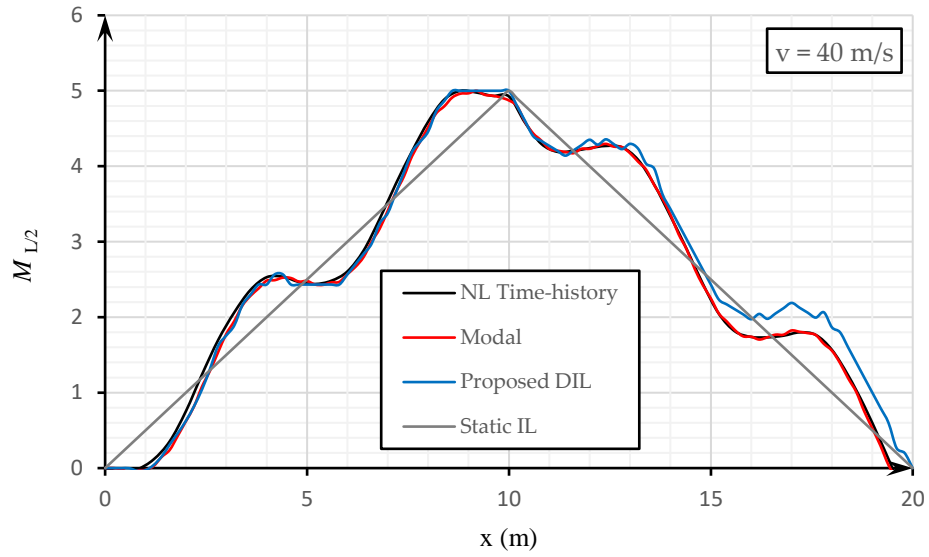
(b)
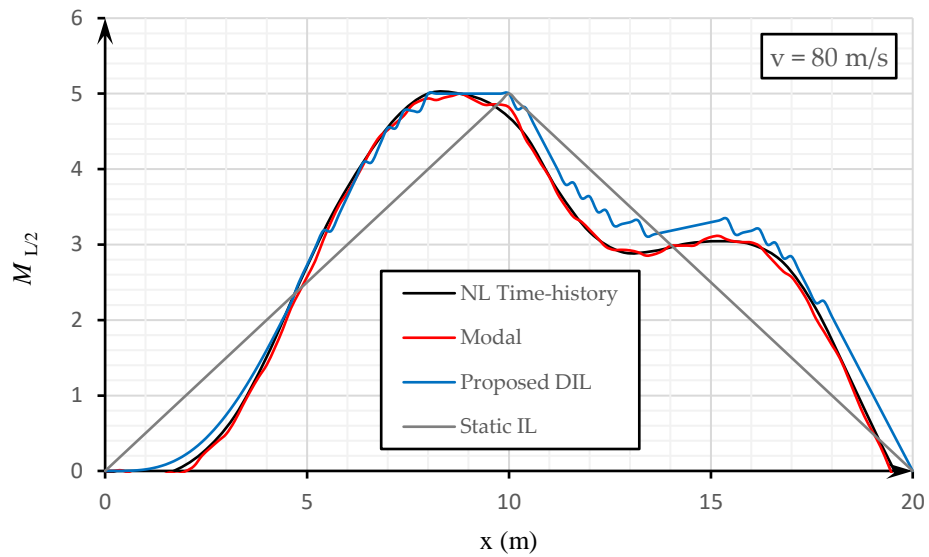
(c)

Fig. 9. Variation of the mid-span moment during the load passage with the speed of: (a) 20 m/s; (b) 40m/s; (c) 80 m/s

3.2. Statically indeterminate structures

Two statically indeterminate beams shown in Fig. 10 are analysed under a single moving load. The goal is to assess how the present method works for statically indeterminate structures as well.
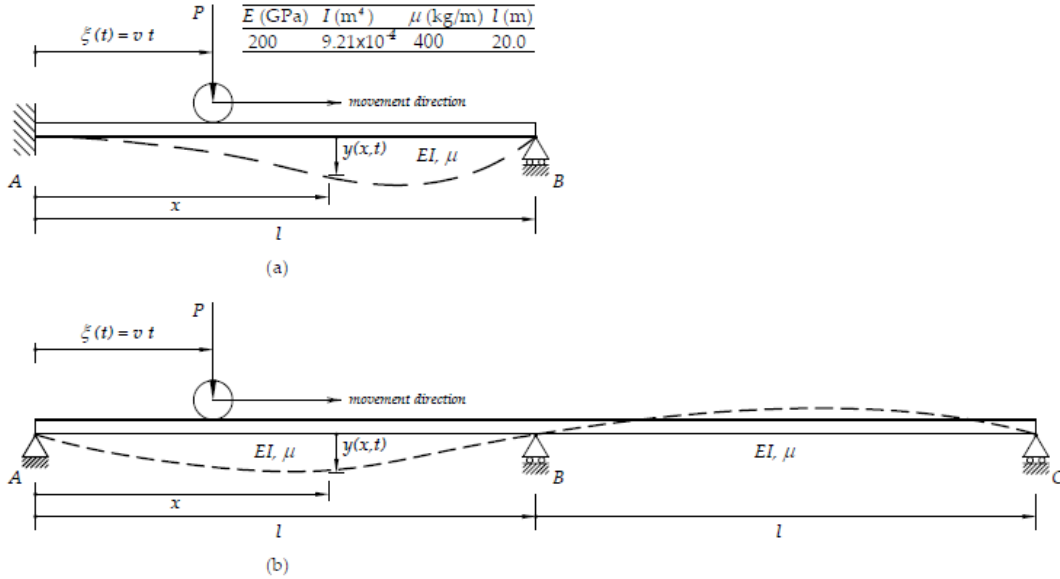
Fig. 10. Two statically indeterminate beams under a single moving load

3.2.1. Example 2

A similar study was performed on a fixed-simple support beam as shown in Fig. 10(a). The exact modes of vibration of a simple span beam (Fig. 10) given in [44] is rewritten as follows:

$$\phi_i(x) = (\cos \beta_i x - \cosh \beta_i x) - C_{1i}(\sin \beta_i x - \sinh \beta_i x)$$

$$C_{1i} = \frac{\cos \beta_i l - \cosh \beta_i l}{\sin \beta_i l - \sinh \beta_i l}; \quad \beta_1 l = 3.9266; \quad \beta_2 l = 7.0686; \ \dots \tag{20}$$

For determination of the support B reaction using the present method, the corresponding reaction is omitted, see Fig. 11(a), and the modes of vibration of the resulted surrogate beam will be as follows [44]:

$$\phi_{si-R}(x) = (\cos\beta_i x - \cosh\beta_i x) - C_{2i}(\sin\beta_i x - \sinh\beta_i x)$$

(21)

$$C_{2i} = \frac{\cos\beta_i l + \cosh\beta_i l}{\sin\beta_i l + \sinh\beta_i l}; \quad \beta_1 l = 1.8751; \quad \beta_2 l = 4.6941; \dots$$

In addition, for determination of the support A moment, the surrogate beam is a simply supported beam, as shown in Fig. 11(b), with the following modes of vibration:

$$\phi_{si-M}(x) = \sin\frac{i\pi x}{l}$$

(22)

$R(t) = R\,[(\cos\beta_i x\text{-}\cosh\beta_i x)\text{-}C_{2i}\,(\sin\beta_i x\text{-}\sinh\beta_i x)]$

$\phi_{si} = (\cos\beta_i x\text{-}\cosh\beta_i x)\text{-}C_{2i}\,(\sin\beta_i x\text{-}\sinh\beta_i x)$

(a)

$M\sin i\pi x/l$

$\phi_{si} = \sin i\pi x/l$

(b)
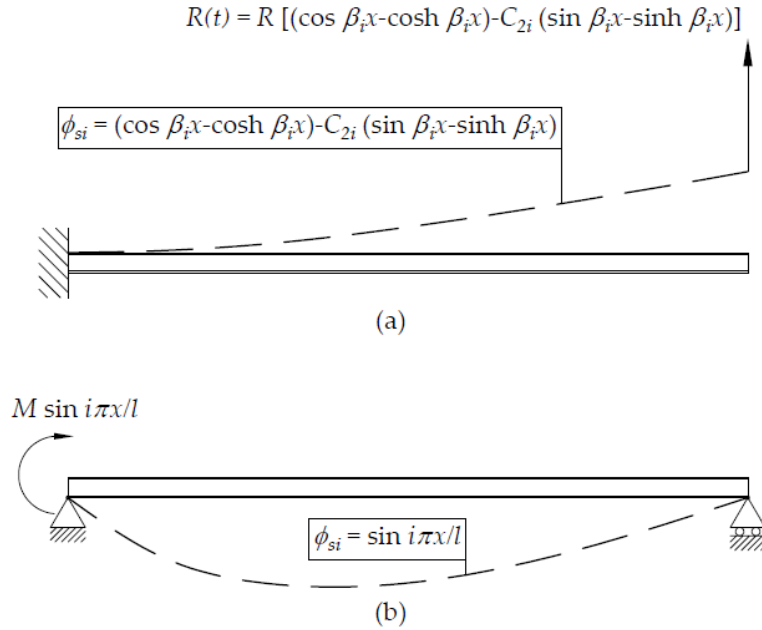
Fig. 11. Surrogate beams for determination of: (a) the support B reaction; (b) the support A moment

Alike Example 1, the sensitivity of the proposed method in terms of various speeds of the moving load is studied for the new end conditions. The results for the support B reaction and the support A moment are illustrated in Figs. (12) and (13), respectively. The accuracy of the method can be observed by comparing the corresponding results with those obtained by the nonlinear time history analysis. As observed by the graphs, the reaction estimated by the modal decomposition method has fluctuation which harden the load identification, while the proposed method provides a smooth curve that fits well to the nonlinear time-history analysis. It should be declared that the results of proposed method were obtained by incorporating the first mode of vibration of the surrogate beam.
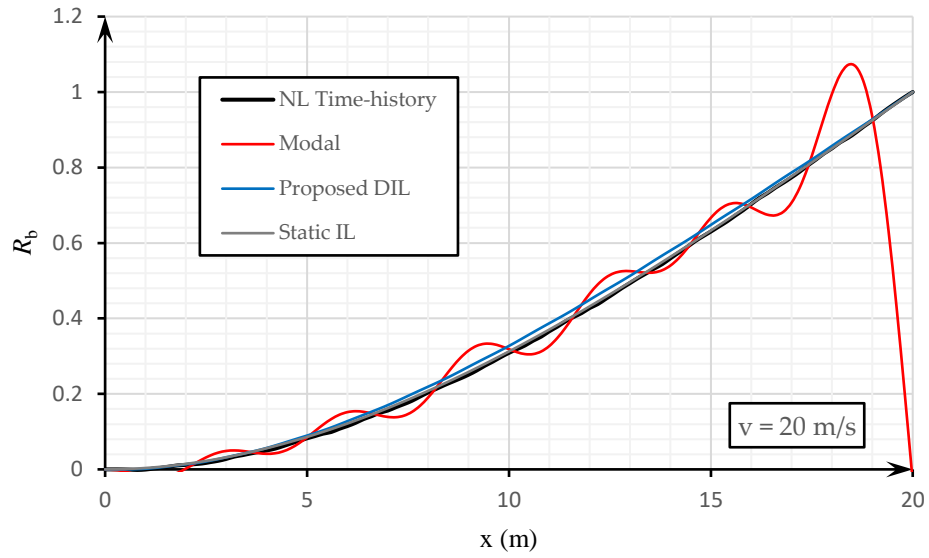
(a)
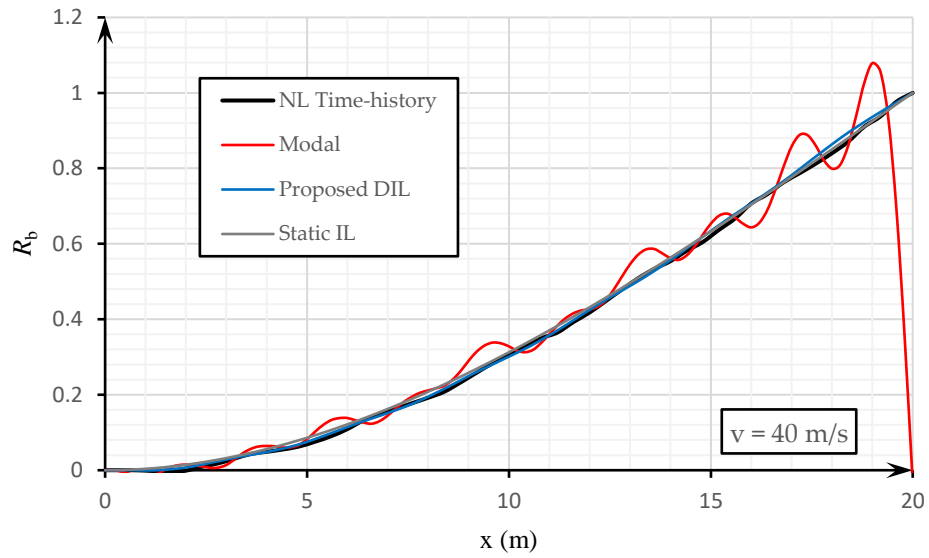
(b)
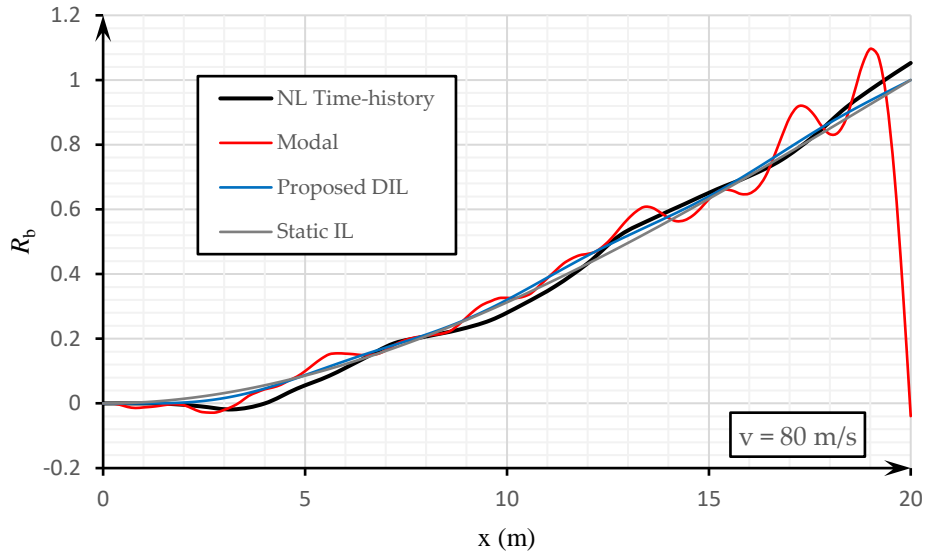
(c)

Fig. 12. Variation of the support B reaction during the load passage with the speed of: (a) 20 m/s; (b) 40m/s; (c) 80 m/s
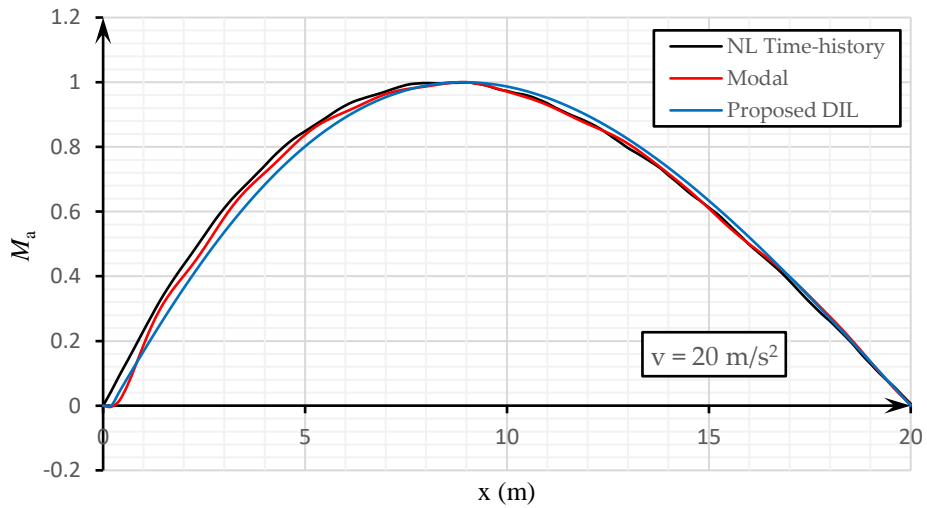
(a)
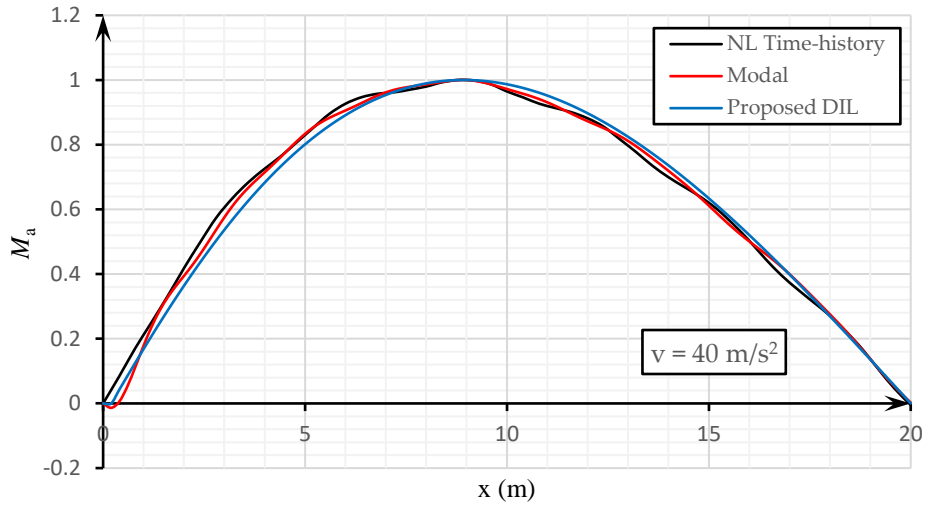
(b)
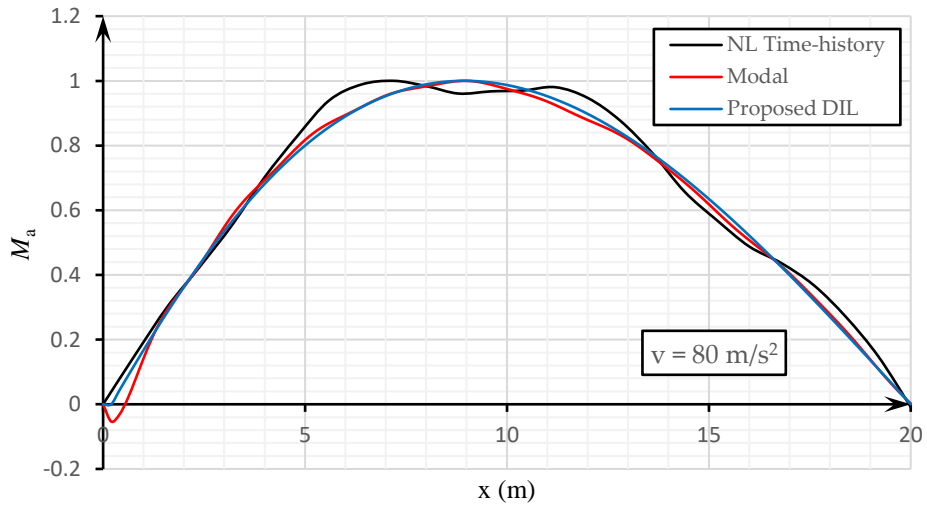
(c)

Fig. 13. Variation of the support A moment during the load passage with the speed of: (a) 20 m/s; (b) 40 m/s; (c) 80 m/s

3.2.2. Example 3

The dynamic influence line of the support B reaction of the 2-span beam under a single load moving with the speed of 40 (m/s) is investigated in the following example (Fig. 10(b)). The surrogate beam related to this reaction is shown in Fig. 14.
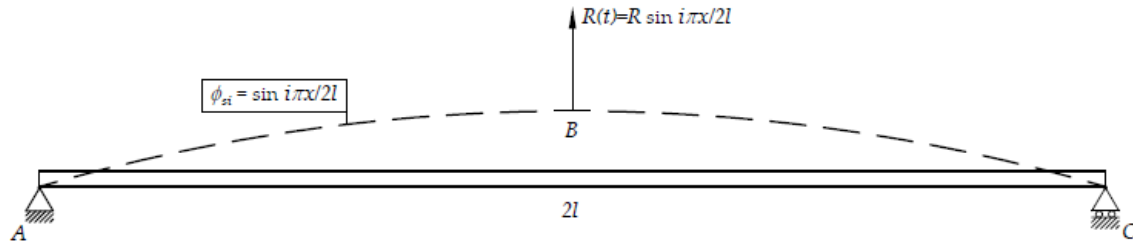
Fig. 14. Surrogate beam for determination of the support B reaction

The results for the reaction at the support B obtained from the proposed method and those resulted from the nonlinear time-history analysis are compared in Fig. 15. The static influence line is also illustrated in Fig. 15. As it is observed, the proposed DIL is converged to the SIL, however it reflects better the effect of dynamic sources.
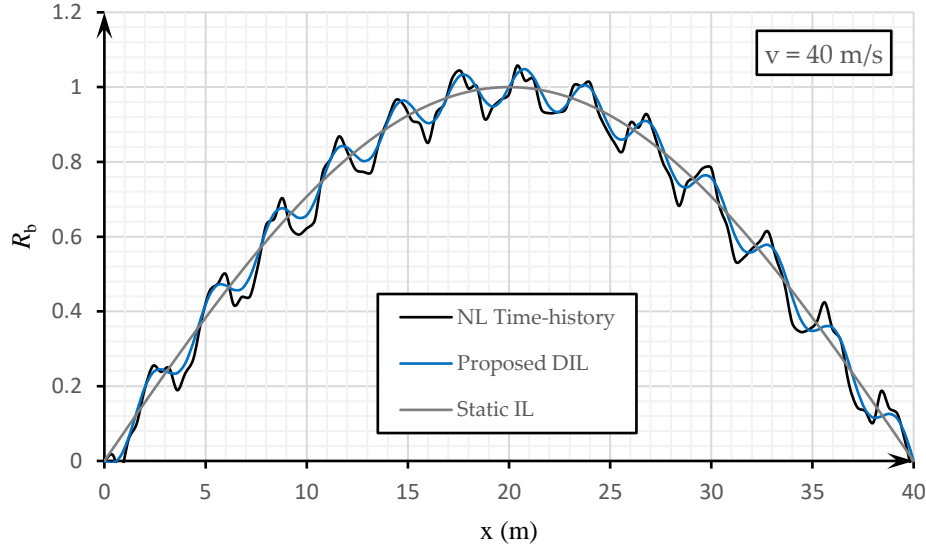
Fig. 15. Variation of the support B reaction determined by different methods

3.4. Singularity assessment

In the modal decomposition method, singularity sources are commonly involved, especially for statically determinate structures. In Example 1, R_b should have a finite value once the load reaches the support B,

22

while it tends to zero for all the modes of vibration since those are sinusoidal. This means that infinite number of modes should be involved to approach the finite value of R_b, making the analysis time consuming. Fig. 16 illustrates the error percentage of 1 m end length of the beam. The figure implies that a large number of modes should be considered to amend singularity issue of the modal decomposition method existing near the support B. On the other hand, such a problem is not observed in the proposed DIL method.
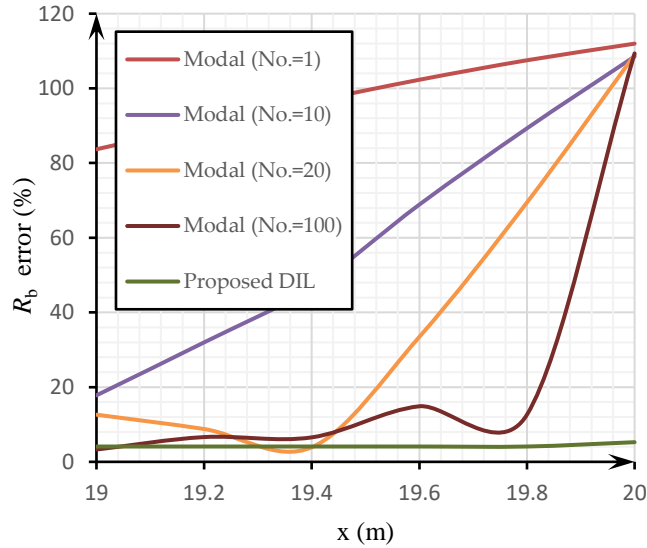
Fig. 16. Analysis error adjacent to the beam end

3.5. Example 4: A two-axle moving load

This example is based on a laboratory test carried out by Yang et al. [25]. In this test, a model two-axle load is considered to move along a 2 m long beam with the speed of 0.25 m/s, as shown in Fig. 17. The beam has a cross-sectional area of 10x150 mm². The moving load weighs 9.38 kg, equally divided between the front and rear axles. The strain response of the beam's bottom face was monitored at different locations along the beam length. However, the results obtained at the mid-span, shown in Fig. 17, were taken as a base to evaluate the present method efficiency in prediction of the beam response under moving load. The response of the beam was evaluated by combination of the DILs of the front and rear axles shown in Fig. 17 by the grey curves. It was observed that the evaluated response fits well with the results of simulation and has a good agreement with the test data obtained by Yang et al. [25]. The details of the evaluation using the proposed DIL method is described in the next section.
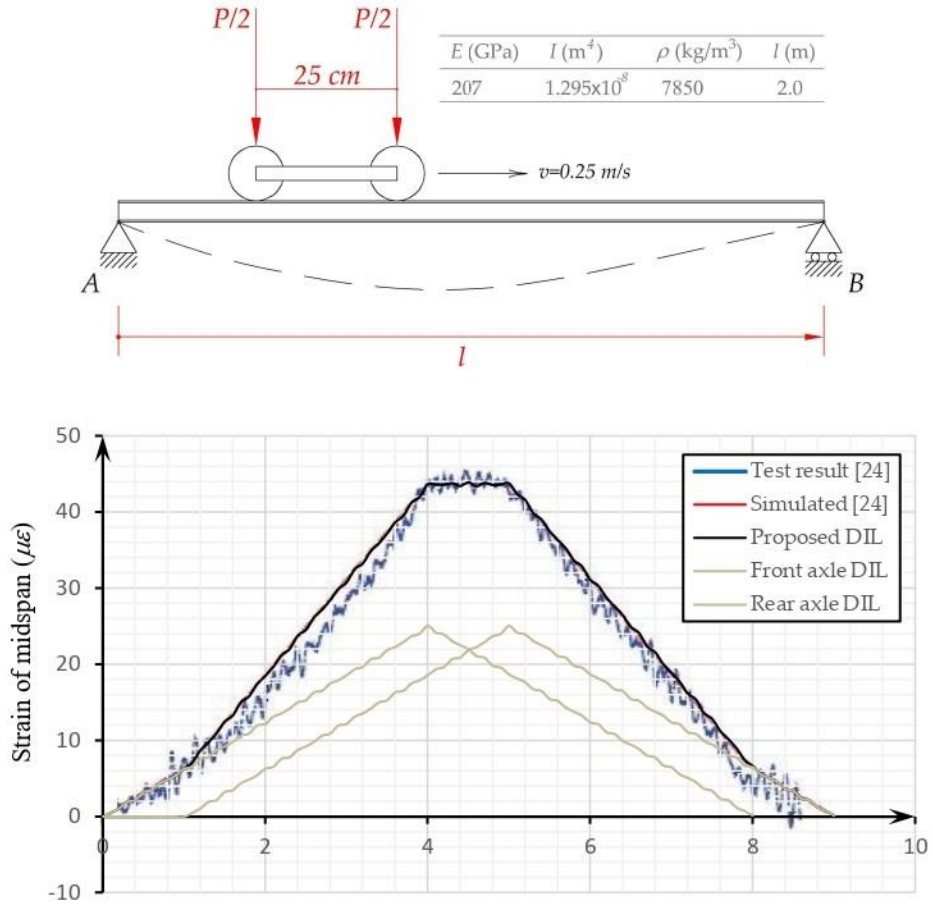
Fig. 17. Verification of the present method by comparing with test data [25]

4. Generalisation of load identification using the proposed DIL method

Based on the previous examples, a flowchart is outlined for the identification of a multi-axle moving load, as shown in Fig. 18.
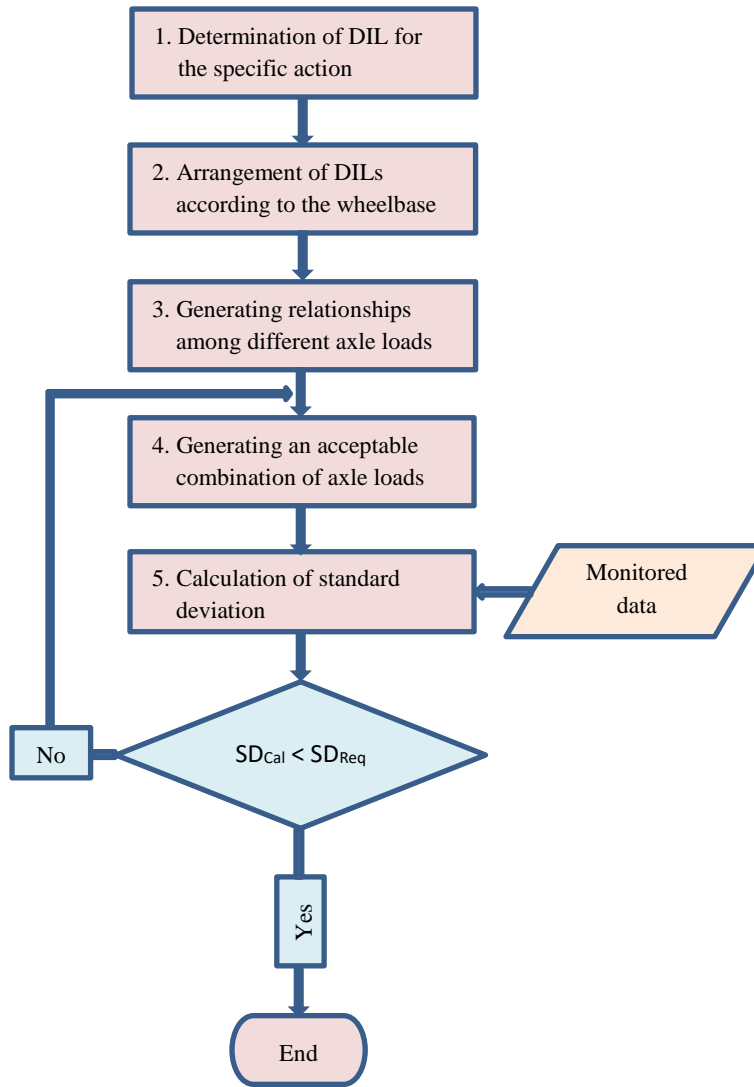
Fig. 18. Flowchart of moving load identification

4.1. Description of the flowchart steps

Step 1: Similar to the Examples 1-3, the DIL of the required reaction of the beam is determined depending on the support conditions and the load speed.

Step 2: *N* similar DILs, where *N* is the number of axles, are arranged at a distance equal to the wheelbase (see Fig. 19).

Step 3: At least, N relationships can be developed among different axle loads as follows. These relationships are regarded as constraints for identification of the moving loads.

$$R_i = DIL_i \left(P_i + P_{i+1} \right) \quad for\ i = 1, 2, \dots, N \tag{23}$$

Step 4: According to the above-mentioned relationships, a set of acceptable axle loads are predicted, i.e.,

$$\mathbf{P} = \{P_1, P_2, \dots, P_N | R_i = DIL_i \ (P_i + P_{i+1}) \quad for \ i = 1,2,\dots,N\}$$

(24)

Step 5: The response of the beam under the predicted multi-axle moving loads is determined as follow:

$$R_{Pred} = \sum_{i=1}^{N} (DIL_{Pi}) \ P_i$$

(25)
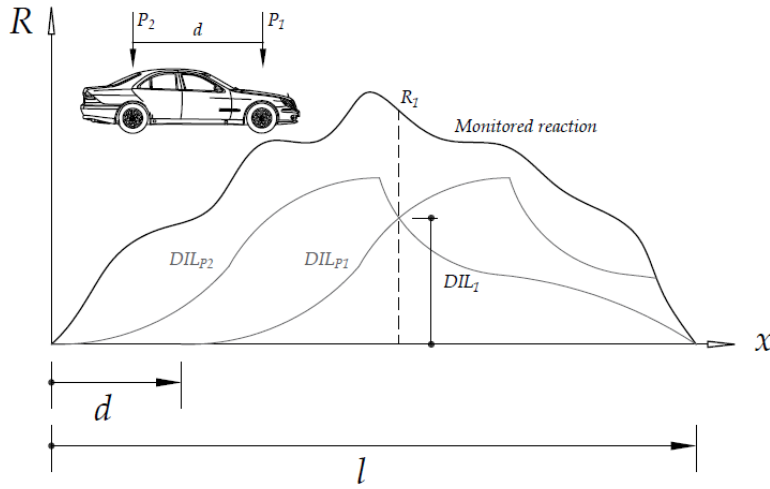
Fig. 19. Application of DIL method for moving load identification

The standard deviation of the predicted response is evaluated in comparison to the monitored data (or simulated data as utilised in this paper). If the calculated SD satisfies the required SD, the identification process is terminated. Otherwise, the process should be executed again from *Step 5* by assuming another set of acceptable axle loads. An application of the method is conducted in the following example.

4.2. Example 5: Evaluation of the axle loads of a two-axle vehicle

A two-axle vehicle is considered to pass along a simply supported beam with the speed of 40 m/s (144 km/h), as shown in Fig. 20. The front and rear axles weigh 7 kN and 5 kN, respectively.
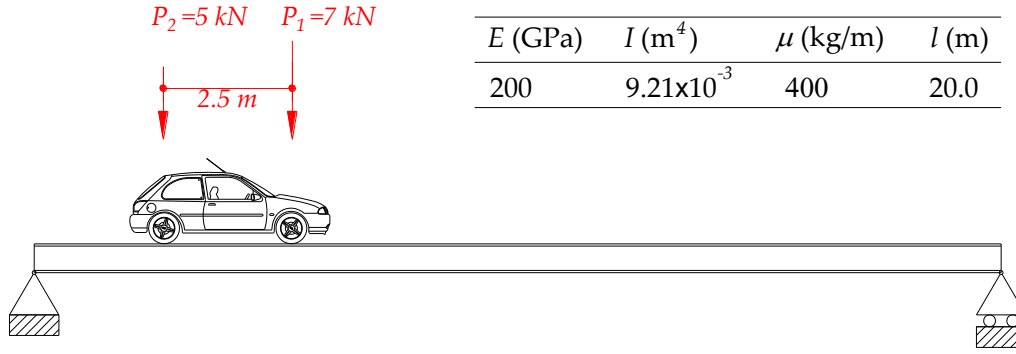
Fig. 20. A two-axle vehicle moving on a simple supported beam

A nonlinear time-history analysis was conducted in SAP2000 [43]. The corresponding results for the mid-span moment during the time of passage, shown in Fig. 21, are taken as a benchmark to find out the accuracy of the present method. In Fig. 21, the two grey curves depict the dynamic influence lines of mid-span moment, as obtained in Example 1, with 0.0625 (s) time difference denoting the distance between the axles.
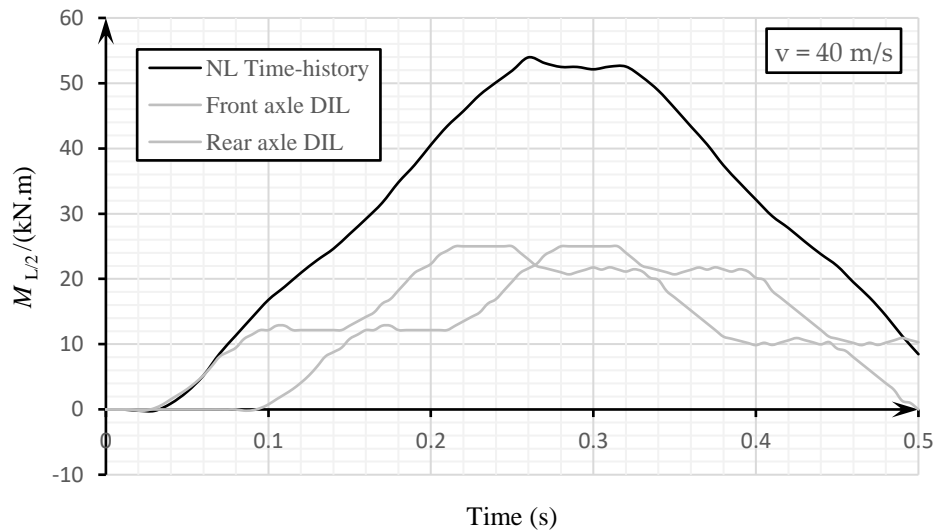
Fig. 21. Mid-span moment during the time obtained by nonlinear time-history analysis

To estimate the mid-span moment using the present method, a linear combination of the mid-span dynamic influence lines of two axles are used as follows:

$$M_{L/2} = (DIL_{P_1}) P_1 + (DIL_{P_2}) P_2$$

(26)

27

in which $M_{L/2}$ is the mid-span moment during the time measured in site or obtained from the nonlinear time-history analysis in this paper; (DIL_{P_1}) and (DIL_{P_2}) are the magnitude of the dynamic influence lines obtained from the present method as illustrated in Example 1; and P_1 and P_2 are, respectively, the front and rear axle loads which are assumed to be unknown.

In this example, the intersection of the dynamic influence lines is an appropriate point to determine the sum of the axle loads because (DIL_{P_1}) and (DIL_{P_2}) are the same and $P_1 + P_2$ is equal to 12.08 kN, hence with less than 0.6% error.

For the next step, a variety of values for P_1 and P_2 is considered provided that their summation is 12.08 kN. In each case, the correlation between the nonlinear time-history diagram and that resulted from the present method is evaluated based on the standard deviation. The results are presented in Fig. 22. It is obtained that the least standard deviation is attained as P_1 and P_2 equal 7.04 kN and 5.04 kN, respectively. The results anticipated by the present method has 0.8% error, approximately.
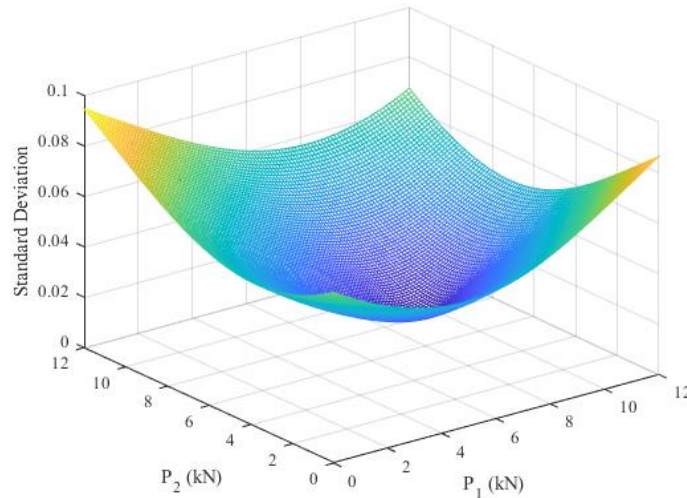
Fig. 22. Standard deviation in terms of different values of axle loads

The accuracy of the results from the present method and those obtained from the nonlinear time-history analysis are depicted in Fig. 23. An appropriate correlation exists between the corresponding responses.
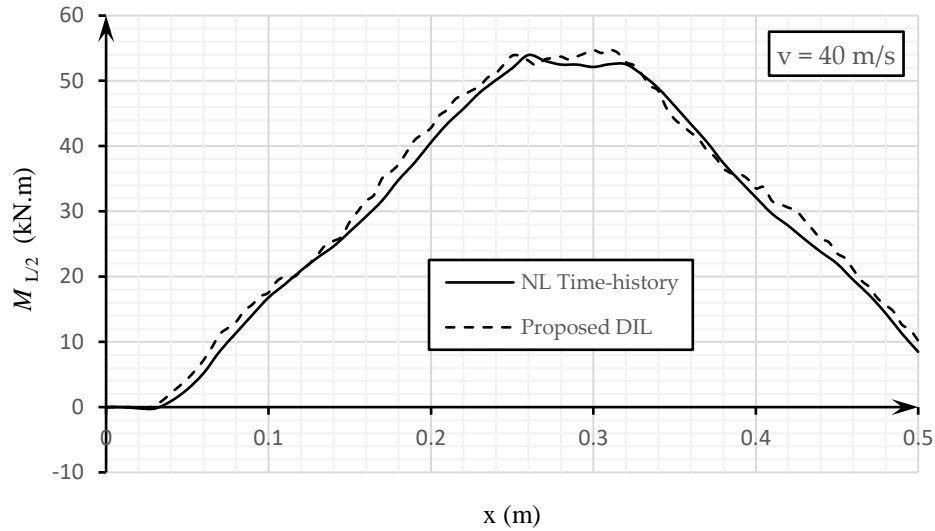
Fig. 23. Mid-span moment during the time

4.3. Example 6: case study with field data

In this section a case study is considered for the validation of the proposed method using real field data. The case study corresponds to an instrumented Network Rail E-type steel half-through railway bridge. This structure has a single skew span of 26.82 m carrying two rail lines within the West Coast Main Line near the city of Crewe in the United Kingdom. The primary structural components of the bridge include two steel longitudinal girders, steel transversal beams, and a reinforced concrete (RC) deck. The longitudinal girders are I-shaped steel plates, precambered and 2.2 meters deep, simply supported by RC abutments at both ends. The transversal beams, which provide lateral strength and stability, are universal column (UC) sections with a depth of 0.368 meters. The deck is a composite structure 0.250 meters deep, featuring a double layer of steel reinforcement. For a comprehensive description of the structural system and visualization of the sensor data within a BIM environment, readers can refer to sources [45, 46].

The sensing system installed in the bridge has unique monitoring features, as it was designed to be used both during construction and operation and was integrated during the construction phase. Implementing the sensing system from the conceptual design stage addresses a critical gap for developing a digital twin and understanding the undamaged structural integrity of the bridge, providing a valuable baseline for future comparisons throughout its operational life [47]. This early-stage instrumentation included fibre-optic-based strain and temperature Fibre Bragg Grating (FBG) sensors installed along the flanges of the main steel girders and the concrete deck. Additionally, extra sensors for detecting accelerations were added in the first half of 2021, along with a new centralised data acquisition system [48]. Such monitoring system

29

has enabled the development of an online platform for the continuous monitoring of the structural health of the bridge, equipped with several features such a real-time B-WIM system [49], among others. For this study, the strain deformation data recorded by the FBG sensors at the main steel girders is used, specifically during the crossing of a New Measurement Train (NMT) because the weight and layout of the axles are precisely known. In particular, a NMT crossing (03.03.2022 15:13:43 UTC) with 28 axles, a total weight of 332.84 Tons and an average speed of 84.03 mph is considered in the following. The full description of the bridge and monitoring system can be found in Refs. [48] and [49].

The midspan deflection of the main girder monitored by the B-WIM system is illustrated in Fig. 24. According to Fig. 24, the train entered the bridge at, approximately, 14.9 s and passed it completely at about 19.5 s. Consequently, the following dynamic analysis was performed for about 5 seconds.
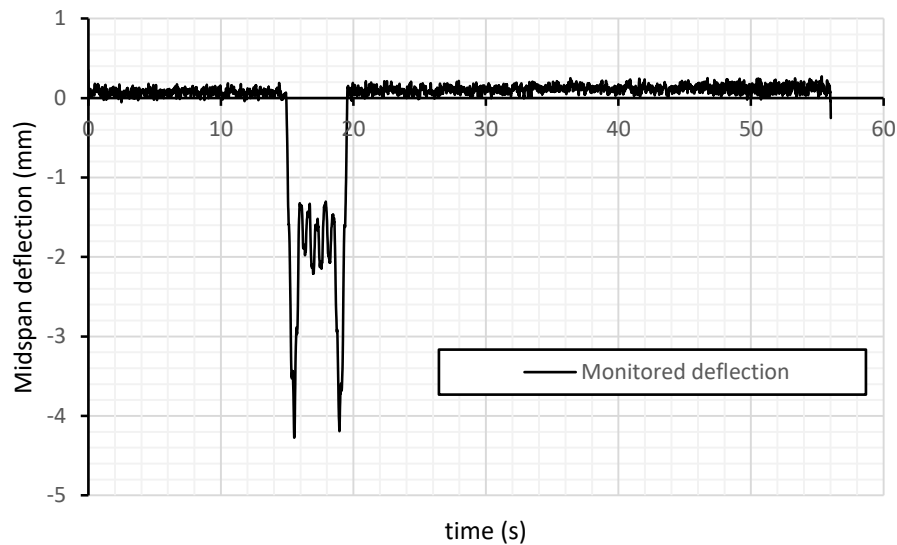
Fig. 24. Midspan deflection during the time

The corresponding midspan moment was obtained based on the monitored deflections. Indeed, the moment was calculated with the well-known formula $M=EI\ d^2y/dx^2$ using the finite difference method. The results are shown in the following figure. It should be noted that for this calculation, the bridge moment of inertia ($=3.8\times10^7$ cm^4 as a double I-shaped section) was multiplied by a modifier of 0.75 to take the load eccentricity into account. The modifier 0.75 is derived assuming the load is located at the ¼ width of section from the west girder.
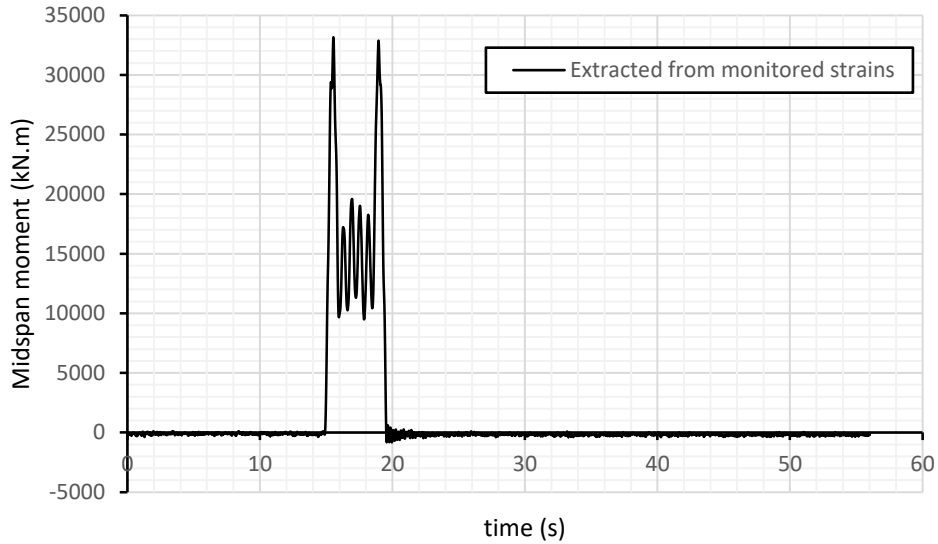
Fig. 25. Midspan moment during the time

For using the proposed dynamic method, the bridge was simplified to a simple support-single span beam element. Then, the dynamic influence line of the midspan moment is derived as shown in Fig. 26. However, to verify the accuracy of this simplification, the midspan moment derived by the simplified model (1D model) is compared, in Fig. 26, with that obtained by modelling the bridge as a 2D model using SAP2000 [43] software. As inferred from Fig. 26, the resulting curves are so close to each other. Accordingly, the 1D model is used for next analyses.
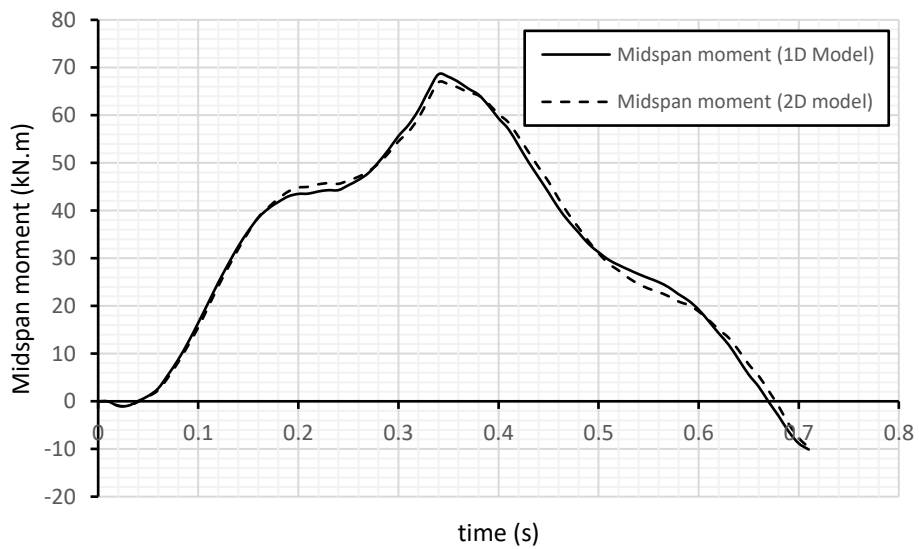
Fig. 26. DIL of mid-span moment (velocity=37.6 m/s)

31

Since the train has 28 axles, 28 DILs with specific time intervals (which are derived by dividing the distance between to consequent axles by the train velocity) are arranged. The midspan moment during the time (5 seconds, approximately) or midspan moment DIL is obtained by the sum of 28 arranged DIL multiplied by the corresponding axle weight. The results obtained by the proposed DIL method is given in Fig. 28 in comparison to the corresponding results derived based on the monitored displacements.
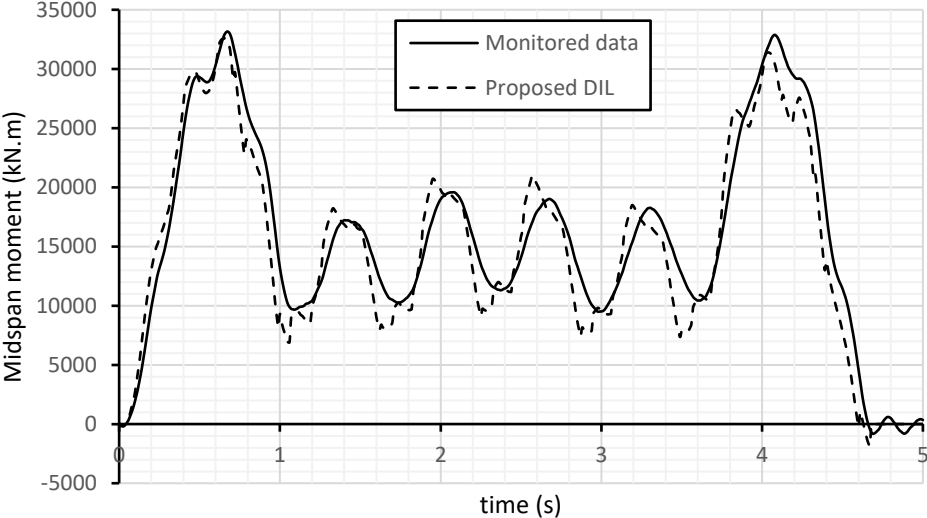
Fig. 27. Comparison between the monitored and predicted data

As observed, the estimated dynamic response is in good accordance to the monitored data regarding the maximum moment. Moreover, the figure shows that the proposed DIL method, as a practical method, is able to estimate the variation of the required reactions during the time. To quantify the accuracy of the predicted data, the cumulative errors of the proposed method were evaluated at extremums, and the results are illustrated in Fig. 28. The maximum and the average errors are 9.4% and 3.3%, respectively.
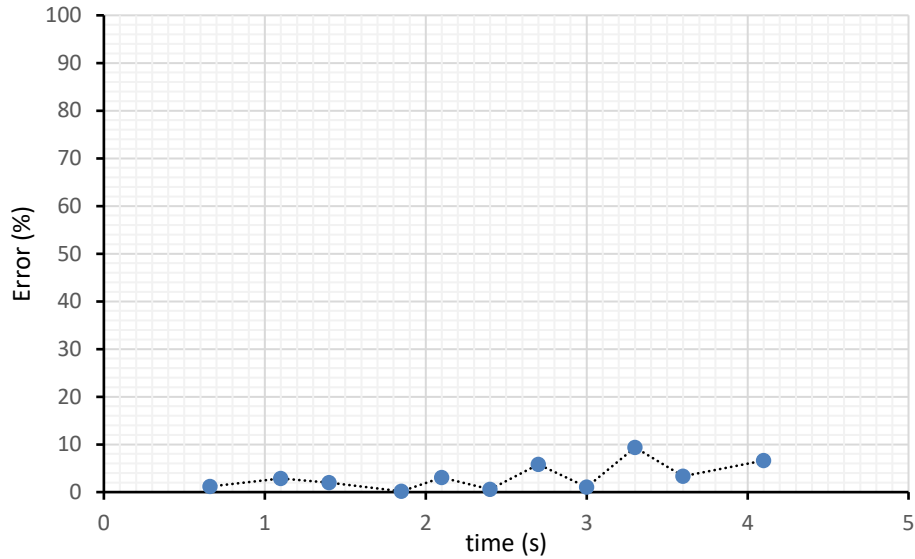
Fig. 28. Error of the data predicted by the proposed DIL method

5. Concluding remarks

This paper develops a method based on a well-known structural engineering concept to solve the ill-conditions existing in the moving load identification and its singularity consequences. In the proposed method the bridge-vehicle dynamic problem is replaced by a surrogate structural system under a dynamic point load. Since the modal shape functions and the assumed dynamic load function are weakened, the source of singularities is eliminated. The accuracy of the method was examined via three types of examples. The first example was related to identification of a one-axle vehicle moving along a simply supported beam as a statically determinate problem. The moving load speed varied from 20 m/s to 80 m/s single beam. The workability of the present method for statically indeterminate structures was evaluated through the second example, which was same as the first one except that one of the supports was assumed to be fixed. The ability of the proposed method in the identification of a two-axle vehicle moving along a simply supported beam was investigated through the third example. Finally, the method was examined based on the data monitored by a real bridge weigh-in-motion system. The main findings are summarised as follows:

1. Using the weakened shape functions, acceptable results were achieved by considering the only possible shape function of the surrogate beam in case the original beam is statically determinate. For the statically indeterminate beams , the first shape function of the surrogate beam provides adequate accuracy in load identification.

33

2. For simply supported beams, the moving load is estimated with an error of less than 5% by taking only a linear shape function (as the only possible shape function) for a surrogate beam. While, in the modal decomposition method, such accuracy is obtained by using more than 20 modal shape functions. The numerous shape functions make the load identification more complicated.

3. The proposed method also worked well for the statically indeterminate beams.

4. The front and rear axle loads of a two-axle vehicle moving along a simply supported beam was estimated with less than 1% error.

5. The midspan moment predicted by the proposed method agree well with the data monitored by the B-WIM system installed on a real bridge. The maximum and the average errors were 9.4% and 3.3%, respectively.

6. It should be noted that although the present method was employed on the uniaxial superstructures using the dynamic influence line, it can readily be generalized to the biaxial superstructures using the concept of the dynamic influence area.

According to the accurate and reliable results obtained from the present method, it can be regarded as a simple and practical way for identification of moving loads. However, it should be noted that the effect of any sources of noise is not addressed in this paper and will be studied in subsequent studies.

Acknowledgements

References

[1] Kozin F, Natke HG. System identification techniques. Structural Safety 1986; 3:269-316.

[2] Yu L, Chan THT. Recent research on identification of moving loads on bridges. J Sound Vib 2007; 305:3-21.

[3] O'Connor C, Chan THT, Dynamic loads from bridge strains, J Struct Eng ASCE 1988; 114:1703–1723.

[4] Chan THT, Law SS, Yung TH, Yuan XR. An interpretive method for moving force identification, J Sound Vib 1999; 219(3):503–524.

[5] Law SS, Chan THT, Zeng QH, Moving force identification: a time domain method, J Sound Vib 1997; 201(1): 1–22.

[6] Law SS, Chan THT, Zeng QH, Moving force identification: a frequency and time domains analysis, J Dyn Syst Meas ASME 1999; 12 (3):394–401.

[7] Yu L, Chan THT. Moving force identification based on the frequency–time domain method, J Sound Vib 2003; 261(2):329–349.

[8] Liu J, Meng X, Jiang C, Han X, Zhang D. Time-domain Galerkin method for dynamic load identification Jie. Int J Numer Meth Eng 2016; 105:620–40.

[9] Sun Y, Luo L, Chen K, Qin X, Zhang Q. A time-domain method for load identification using moving weighted least square technique. Comput and Struct 2020; 234:1-21.

[10] Zhou HC, Li HN, Yang DH, Yi TH. Moving force identification of simply supported bridges through the integral time domain method. J Sound Vib 2022; 534:117046.

[11] Jiang XQ, Hu HY, Reconstruction of distributed dynamic loads on an Euler beam via mode-selection and consistent spatial expression, J Sound Vib 2008; 316:122–136.

[12] Pinkaew T, Identification of vehicle axle loads from bridge responses using updated static component technique, Eng Struct 2006; 28:1599-1608.

[13] González A, Rowley C, Obrien EJ, A general solution to the identification of moving vehicle forces on a bridge, Int J Numer Methods Eng 2008; 75:335–354.

[14] Dowling J, Obrien EJ, Gonz´alez A, Adaptation of cross entropy optimisation to a dynamic bridge WIM calibration problem. Eng Struct 2012; 44:13–22.

[15] Feng D, Sun H, Feng MQ, Simultaneous identification of bridge structural parameters and vehicle loads. Comput Struct 2015; 157:76–88.

[16] Jia Y, Yang Z, Song Q, Experimental study of random dynamic loads identification based on weighted regularization method. J Sound Vib 2015; 342:113–123.

[17] Li Q, Lu Q, A revised time domain force identification method based on Bayesian formulation. Int J Numer Methods Eng 2019; 118:411–431.

[18] Li X, Zhao H, Chen Z, Wang Q, Chen J, Duan D, Force identification based on a comprehensive approach combining Taylor formula and acceleration transmissibility. Inverse Probl Sci Eng 2018; 26:1612–1632.

[19] Qiao B, Mao Z, Liu J, Zhao Z, Chen X, Group sparse regularization for impact force identification in time domain. J Sound Vib 2019; 445:44–63.

[20] Li H, Liu B, Huang W, Liu H, Wang G. Vibration load identification in the time-domain of high arch dam under discharge excitation based on hybrid LSQR algorithm. Mechanical Systems and Signal Processing. 2022 Sep;177:109193.

[21] Chen Z, Wang Z, Wang Z, Chan THT. Comparative studies on the criteria for regularization parameter selection based on moving force identification. Inverse Probl Sci Eng 2021; 29:153-173.

[22] Zhu XQ, Law SS. Moving loads identification through regularization. J Eng Mech ASCE 2002, 128(9):989-1000.

[23] Chen Z, Chan THT. A truncated generalized singular value decomposition algorithm for moving force identification with ill-posed problems. J sound Vib 2017; 401: 297-310.

[24] Chen Z, Deng L, Kong X. Modified truncated singular value decomposition method for moving force identification. Adv Struct Eng 2022; 25 (12).

[25] Yang H, Yan W, He H. Parameters identification of moving load using ANN and dynamic strain. Shock Vib 2016; 8249851.

[26] Liu B, Li H, Wang G, Huang W, Wu P, Li Y. Dynamic material parameter inversion of high arch dam under discharge excitation based on the modal parameters and Bayesian optimised deep learning. Advanced Engineering Informatics. 2023 Apr 1;56:102016–6.

[27] Paul D, Roy K. Application of bridge weigh-in-motion system in bridge health monitoring: a state-of-the-art review. Struct Health Monit 2023; 22(6):4194-4232.

[28] Moses F. Weigh-in-motion system using instrumented bridges. Transp Eng J ASCE 1979; 105(3): 233–249.

[29] Chan THT, Ashebo DB. Theoretical study of moving force identification on continuous bridges. J Sound Vib 2006; 295:870-883.

[30] Wang N, Ren W, Li M. Identification of bridge moving loads based on influence lines. J Vib Shock 2013; 32(2):129-133.

[31] Wang NB, He LX, Ren WX, Huang TL. Extraction of influence line through a fitting method from bridge dynamic response induced by a passing vehicle. Eng Struct 2017; 151:648-664.

[32] Asnachinda P, Pinkaew T. Vehicle Axle Load Identification Using Extracted Bridge Influence Line via Updated Static Component Technique, Eng J 2021; 25:45-60.

[33] Yang J, Hou P, Yang C, Zhang Y. Study on the Method of Moving Load Identification Based on Strain Influence Line. Appl Sci 2021; 11(2):853-868.

[34] Qian CZ, Chen CP, Hong L, Dai LM. Axle load identification of moving vehicles based on influence lines of bridge bending moment. Nonlinear Eng 2014; 3(3):125-131.

[35] Filho FV. Dynamic Influence Lines of Beams and Frames. Journal of the Structural Division. 1966 Apr 1;92(2):371–86.

[36] Åkesson BÅ. Harmonic influence lines in structural dynamics calculated by use of Müller-Breslau's theorem. Journal of Sound and Vibration. 1990 Oct;142(1):1–13.

[37] Wattanasakulpong N, Karamanli A, Vo TP. Nonlinear dynamic response of FG-GPLRC beams induced by two successive moving loads. Engineering Analysis with Boundary Elements. 2023 Dec 2;159:164–79.

[38] Songsuwan W, Wattanasakulpong N, Kumar S. Nonlinear transient response of sandwich beams with functionally graded porous core under moving load. Engineering Analysis with Boundary Elements. 2023 Jun 7;155:11–24.

[40] Wattanasakulpong N, Eiadtrong S. Transient Responses of Sandwich Plates with a Functionally Graded Porous Core: Jacobi–Ritz Method. International Journal of Structural Stability and Dynamics. 2022 Aug 8;23(04).

[41] Songsuwan W, Wattanasakulpong N, Vo TP. Nonlinear vibration of third-order shear deformable FG-GPLRC beams under time-dependent forces: Gram–Schmidt–Ritz method. Thin-Walled Structures. 2022 Jul;176:109343.

[42] Chaikittiratana A, Wattanasakulpong N. Gram-Schmidt-Ritz method for dynamic response of FG-GPLRC beams under multiple moving loads. Mechanics Based Design of Structures and Machines. 2020 Jun 29;50(7):2427–48.

[43] CSI, SAP2000, Integrated Software for Structural Analysis and Design, Computers and Structures Inc., Berkeley, California.

[44] Rao SS. Vibration of continuous systems. John Wiley & Sons; 2019.

[45] Davila Delgado JM, Butler LJ, Brilakis I, Elshafie MZEB, Middleton CR. Structural Performance Monitoring Using a Dynamic Data-Driven BIM Environment. Journal of Computing in Civil Engineering. 2018 May;32(3).

[46] Lin W, Butler LJ, Elshafie MZEB, Middleton CR. Performance Assessment of a Newly Constructed Skewed Half-Through Railway Bridge Using Integrated Sensing. Journal of Bridge Engineering. 2019 Jan;24(1):04018107.

[47] Gürdür Broo D, Bravo-Haro M, Schooling J. Design and implementation of a smart infrastructure digital twin. Automation in Construction. 2022 Apr;136:104171.

[48] Fidler P, Huseynov F, Bravo Haro M, Vilde V, Schooling J, Middleton C. Augmenting an existing railway bridge monitoring system with additional sensors to create a bridge weigh-in-motion system and digital twin. In SHMII-11. 11th International Conference on Structural Health Monitoring of Intelligent Infrastructure, 2022.

[49] Huseynov F, Fidler P, Bravo Haro M, Vilde V, Schooling J, Middleton C. Setting up a real-time train load monitoring system in the UK using bridge weigh-in motion technology-a case study. In SHMII-11: 11th International Conference on Structural Health Monitoring of Intelligent Infrastructure, 2022.